

## Modelling the biological treatment process aeration efficiency: application of the artificial neural network algorithm

Mpho Muloiwa<sup>a,\*</sup>, Megersa Dinka<sup>b</sup> and Stephen Nyende-Byakika<sup>a</sup>

<sup>a</sup> Department of Civil Engineering, Tshwane University of Technology, Private Bag X680, Pretoria 0001 Staatsartillerie Road, Pretoria West, South Africa

<sup>b</sup> Department of Civil Engineering Science, University of Johannesburg, Auckland Park Campus 2006, Box 524, Johannesburg, South Africa

\*Corresponding author. E-mail: muloiwam@yahoo.com

### ABSTRACT

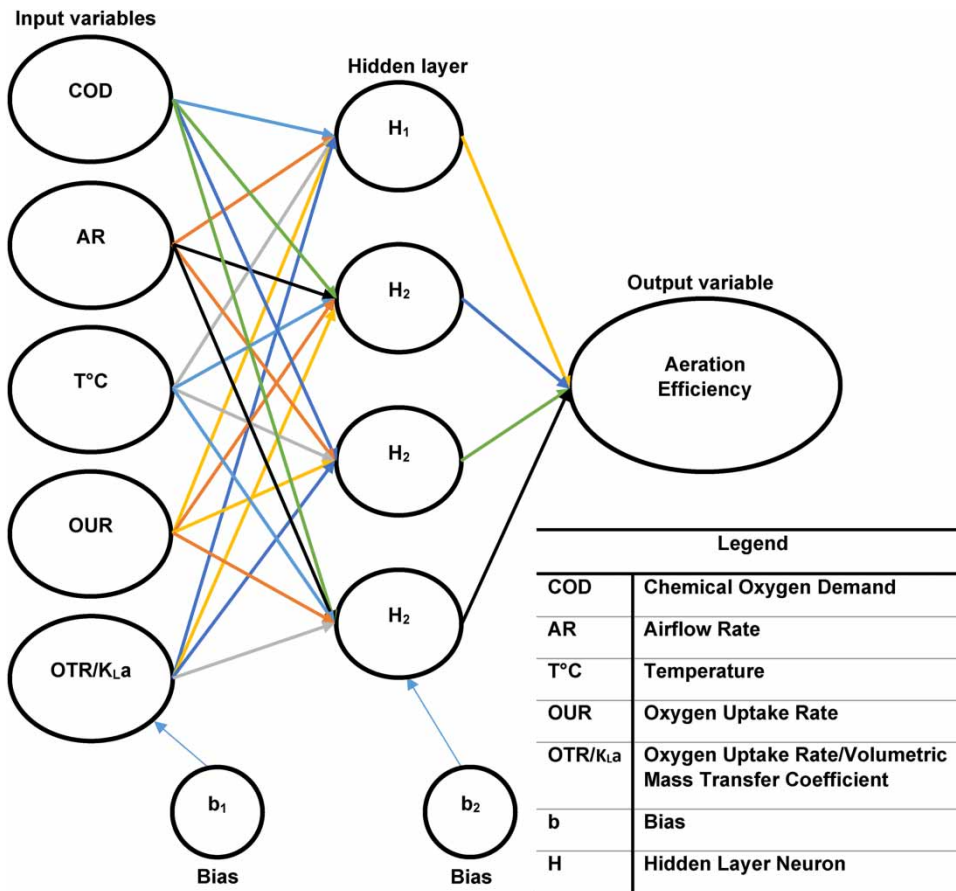
The biological treatment process (BTP) is responsible for removing chemical oxygen demand (COD) and ammonia using microorganisms present in wastewater. The BTP consumes large quantities of energy due to the transfer of oxygen using air pumps/blowers. Energy consumption in the BTP is due to low solubility of oxygen, which results in low aeration efficiency (AE). The aim of the study was to develop an AE model that can be used to monitor the performance of the BTP. Multilayer perceptron artificial neural network (MLP ANN) algorithm was used to model AE in the BTP. The performance of the AE model was evaluated using  $R^2$ , mean square error (MSE), and root mean square error (RMSE). Sensitivity analysis was performed on the AE model to determine variables that drive AE. The results of the study showed that MLP ANN algorithm was able to model AE.  $R^2$ , MSE, and RMSE results were 0.939, 0.0025, and 0.05, respectively, during testing phase. Sensitivity analysis results showed that temperature (34.6%), COD (21%), airflow rate (19.1%), and OTR/ $K_L a$  (15.7%) drive AE. At high temperatures, the viscosity of wastewater is low which enables oxygen to penetrate the wastewater, resulting in high AE. The AE model can be used to predict the performance of the BTP, which will assist in minimizing energy consumption.

**Key words:** aeration efficiency, airflow rate, COD concentration, oxygen uptake rate, temperature, volumetric mass transfer coefficient

### HIGHLIGHTS

- Aeration efficiency increases with an increase in temperature.
- Aeration efficiency decreases with an increase in airflow rate.
- Temperature and airflow rate are the biggest driver of energy consumption.
- Temperature, COD, and airflow rate control aeration efficiency in the biological treatment process.
- High temperatures and airflow rates improve volumetric mass transfer coefficient.

## GRAPHICAL ABSTRACT



## 1. INTRODUCTION

Wastewater treatment plants (WWTPs) are used all over the world including South Africa (SA). WWTPs are responsible for purifying domestic and industrial wastewater to an acceptable effluent quality before being discharged into the environment (Żyłka *et al.* 2021). The biological treatment process is responsible for decomposing organic matter and oxidising inorganic matter using microorganisms present in wastewater (Kanaujiya *et al.* 2019). The biological treatment process consumes large quantities of energy due to the transfer of oxygen using air pumps/blowers for respiration and survival of microorganisms (Wang *et al.* 2016; Christoforidou *et al.* 2020; Siatou *et al.* 2020). For example, Wang *et al.* (2016) reported that the biological energy consumption in Germany, United States of America (USA), and SA were 0.296 kWh/m<sup>3</sup>, 0.37 kWh/m<sup>3</sup>, and 0.3–0.61 kWh/m<sup>3</sup>, respectively. The energy consumption reported in SA, USA, and Germany accounts for 0.55%, 0.6%, and 0.7%, of the annual electricity consumption in their respective countries. In Spain and Saudi Arabia, biological treatment processes consume 0.8 kWh/m<sup>3</sup> and 1.6 kWh/m<sup>3</sup>, respectively (Christoforidou *et al.* 2020). This energy consumption is high and requires attention in order to achieve low energy consumption.

The high energy consumption in the biological treatment process is due to the fact that oxygen is partially soluble in wastewater, which leads to low aeration efficiency (AE) (Lewis & Whitman 1924). This means that the biological treatment process will not be supplied with sufficient oxygen for respiration of microorganisms due to the resistance of wastewater in transferring oxygen. The low solubility of oxygen in the biological treatment process is caused by the gas liquid film that prevents a gas from dissolving in a liquid as defined by the two film theory (Lewis & Whitman 1924). The viscosity of the wastewater provides the resistance to the passage of oxygen molecules in the biological treatment process, which forces plant managers/operators to aerate 24 h nonstop in order to maintain a high oxygen transfer rate/volumetric mass transfer coefficient (OTR/K<sub>L</sub>a) (Rosso & Stenstrom 2006; Garcia-Ochoa & Gomez 2009; Suresh *et al.* 2009). AE is defined as the ratio of

OTR/ $K_L a$  and the power consumed during the aeration process. AE can be defined by Equation (1).

$$AE = \frac{OTR/K_L a}{P} \quad (1)$$

In order to achieve a high AE, high OTR/ $K_L a$  must be maintained so that oxygen is supplied in the biological treatment process efficiently. To achieve high OTR/ $K_L a$ , research scholars have resorted to high airflow rates in order to penetrate the thickness of the wastewater caused by impurities that provide the resistance of oxygen molecules to dissolve in wastewater (Vogelaar *et al.* 2000; Limpaboon 2013; Shukla & Goel 2018; Zhou *et al.* 2018; Warunyuwong & Imai 2020). Utilizing high airflow rates will increase the air velocity distribution which increases the shear force in the biological treatment process. An increase in the shear force will breakdown the thickness of the wastewater making it possible for oxygen molecules to penetrate and dissolve (Ren *et al.* 2018). According to Zhou *et al.* (2018), an airflow rate of 0.5 vvm (volume of air per volume of liquid per minute) produced 13.21 kg O<sub>2</sub>/h OTR/ $K_L a$ , while an airflow rate of 2 vvm produced 22.43 kg O<sub>2</sub>/h OTR/ $K_L a$ . Similarly, Vogelaar *et al.* (2000) reported that an airflow rate of 0.15 vvm produced 22 kg O<sub>2</sub>/h OTR/ $K_L a$ , while an airflow rate of 0.56 vvm produced 61 kg O<sub>2</sub>/h OTR/ $K_L a$ . It is clear from the literature that high airflow rates will result in high OTR/ $K_L a$ . The challenge with increasing airflow rate to obtain high OTR/ $K_L a$  is that power consumption also increases, resulting in a low AE (Baylar & Bagatur 2000; Pittoors *et al.* 2014; Al Ba'ba'a & Amano 2017; Collivignarelli *et al.* 2019; Du *et al.* 2020; Kan *et al.* 2020). According to Collivignarelli *et al.* (2019), an airflow rate of 100 m<sup>3</sup>/h produced 0.98 kg O<sub>2</sub>/kWh AE, while an airflow rate of 150 m<sup>3</sup>/h produced 0.85 kg O<sub>2</sub>/kWh AE. This is a decrease of 13.3% in AE due to an increase of 33.3% in airflow rate. Similarly, Al Ba'ba'a & Amano (2017) reported that an airflow rate of 0.125 L/min produced 2.8 kg O<sub>2</sub>/kWh AE, while an airflow rate of 0.05 L/min produced 5.2 kg O<sub>2</sub>/kWh AE. This was a decrease of 46.2% in AE due to an increase of 60% in airflow rate. Although high airflow rates improve OTR/ $K_L a$ , they do not benefit AE in the biological treatment process because when high airflow rates are applied, high power consumption are utilized by the air pump/blower. This will result in high energy consumption.

High temperatures, on the other hand, have been reported to improve OTR/ $K_L a$ , which results in an improvement of AE (Krahe *et al.* 1996; Vogelaar *et al.* 2000; Chalasani & Sun 2007; Yang & Park 2012; Pappenreiter *et al.* 2019). This is because at high temperatures, the viscosity of the wastewater decreases, which reduces the thickness of the wastewater and allows oxygen molecules to penetrate and dissolve more rapidly, resulting in high AE (Lewis & Whitman 1924). According to Vogelaar *et al.* (2000), a temperature of 20 °C produced OTR/ $K_L a$  of 17.4 kg O<sub>2</sub> h<sup>-1</sup>, and a temperature of 55 °C produced OTR/ $K_L a$  of 37.4 kg O<sub>2</sub> h<sup>-1</sup>. This is an increase of 53.5% in OTR/ $K_L a$  due to an increase of 63.6% in temperature. Similarly, Yang & Park (2012) reported that a temperature of 13 °C produced OTR/ $K_L a$  of 7 kg O<sub>2</sub>/h while a temperature of 23.5 °C produced OTR/ $K_L a$  of 7.8 kg O<sub>2</sub>/h. This was an increase of 10.3% in OTR/ $K_L a$  due to an increase of 44.7% in temperature. Therrien *et al.* (2019) reported that a temperature of 10 °C produced OTR/ $K_L a$  of 0.0324 kg O<sub>2</sub>/h, and a temperature of 30 °C produced OTR/ $K_L a$  of 0.0376 kg O<sub>2</sub>/h. This was a 13.8% gain in OTR/ $K_L a$  due to a 66.7% increase in temperature. The increase of OTR/ $K_L a$  due to an increase in temperature will result in an increase of AE because no power consumption was increased. An increase in AE will lead to a reducing in energy consumption in the biological treatment process, because low airflow rates can be utilized with high temperatures to achieve a high OTR/ $K_L a$  delivery. The challenge is that the normal operating temperature of wastewater is usually in the range between 18 °C and 22.5 °C (Golzar *et al.* 2020; Tejaswini *et al.* 2020). This low temperature of wastewater will result in a low OTR/ $K_L a$ , which will result in low AE due to high viscosity of the wastewater. Therefore, it is essential to develop a model that can be used to monitor AE in order to achieve low energy consumption in the biological treatment process. The aim of this study was to develop an AE model that can be used to monitor the performance of the biological treatment process. The model will incorporate the effects of temperature variations and airflow rate variations since they drive the efficiency of the biological treatment process. This will assist plant managers/operators in achieving high AE while utilizing low airflow rates that reduce energy consumption in the biological treatment process.

## 2. MATERIALS AND METHODS

### 2.1. Laboratory experiments

Laboratory experiments were carried out at the Tshwane University of Technology, Faculty of Engineering and the Built Environment, Department of Civil Engineering to determine the optimum operating temperature and airflow rate that

improves AE. The airflow rates used were 5 L/min, 10 L/min, 15 L/min, 20 L/min, 25 L/min, and 30 L/min. The airflow rate range was chosen based on the fact that low airflow rate produces low OTR/ $K_L a$  compared with high airflow rates. The low OTR/ $K_L a$  will result in a low AE, whereas high OTR/ $K_L a$  will result in high AE in the biological treatment process. The temperatures used were 15 °C, 17.5 °C, 20 °C, 22.5 °C, 25 °C, 27.5 °C, 30 °C, 32.5, and 35 °C. The temperature range was chosen based on the fact that low temperature result in high viscosity compared with high temperature. The low temperature will result in low AE, whereas high temperature will increase the AE in the biological treatment process. The biological treatment process comprised of the following components: aeration tank, dissolved oxygen (DO) meter and probe, thermostat, air pump, airflow meter, air stone disc bubble diffuser, and a digital wattmeter. The components and the schematic diagram of the biological treatment process are detailed in Table 1 and Figure 1, respectively.

## 2.2. Wastewater collection

Wastewater samples were collected from the Daspoort WWTP bioreactor number two each day. Two samples were collected, one in the morning and one in the afternoon. The collection method (morning and afternoon) was implemented to prevent any biological activity from taking place during the storage process. The APHA (2012) method was used for the collection of wastewater from the Daspoort WWTP. Non sterile powder free nitrile gloves were used to handle all equipment. A 25 L jerry can was used to collect the raw wastewater. An additional 2 L of activated sludge was collected from the return activated sludge. Wastewater samples were collected and aerated within 2 h after collection. After collection, the wastewater was stored in ice bucket at a temperature of 4 °C to make sure that no biological activities take place during transportation to the Tshwane University of Technology, Faculty of Engineering and the Built Environment, Department of Civil Engineering.

## 2.3. Analysis

Chemical oxygen demand (COD) was measured and analysed. The method used for analysing COD was the Standard Methods for the Examination of Water and Wastewater (APHA 2012). COD was analysed using closed reflux colorimetric

**Table 1** | Components of the aeration unit

Components	Type	Remarks
Aeration tank	Circular aeration tank (acrylic material)	10–15 mm thick acrylic material. Dimensions 570 × 300 mm. Total volume is 40 L. Working volume is 30 L
Dissolved oxygen meter and probe	Hanna HI98196 multi-parameter water proof meter	Measures DO, pH, and ORP
Thermostat	Local manufacturer	Controls temperature in the range 0 °C–40 °C
Air pump	Waterfall Resun LP100	Can supply air between 0 and 140 L/min
Airflow meter	MF5712 200 L/min digital gas air nitrogen oxygen mass flow meter	Can measure airflow rate between 0 and 200 L/min
Air stone disc bubble diffuser	Growneer micro pore bubble diffuser	Diffuser is 20 cm in diameter
Digital wattmeter	Geewiz (kilowatt)	Measures power between 0 and 3,600 watts

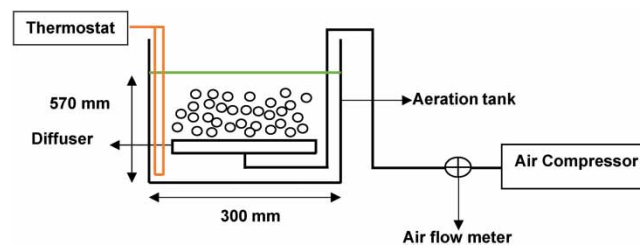


**Figure 1** | Laboratory aeration unit.

(APHA 2012 method 5220). Spectrophotometer (DR3900), digestion vessels, block heater, microburet, and ampule sealer were the equipment used for the analysis.

#### 2.4. Aeration process

Aeration process was conducted twice a day (two samples collected). Two wastewater samples were aerated per day and each sample was aerated for 4 h (hydraulic retention time at Daspoort WWTP). This means that two different temperatures (35 °C and 32.5 °C) were applied during the aeration process at one of the airflow rates (5 L/min) per day. The same process was repeated the following day applying two different temperatures (30 °C and 27.5 °C) and the same airflow rate (5 L/min). The process was then repeated on all temperatures at different airflow rates. A thermostat (Table 1) was used to increase (heat up) the temperature of wastewater from field temperature (18–22.5 °C) to the desired operating temperature. Ice cubes were used to decrease (reduce) the temperature of wastewater from field temperature to the desired operating temperature. Three samples were collected and analysed during each aeration process:

- Initial concentration immediately after collection or before aeration process.
- 2 h concentration.
- 4 h concentration.

#### 2.5. Disposal

After the completion of the aeration process, wastewater was disposed by flushing at the laboratory toilet. The disposal method allows the wastewater to go back to the WWTP.

#### 2.6. Determination of oxygen uptake rate, oxygen transfer rate/volumetric mass transfer coefficient, and aeration efficiency

The dynamic method as described by Garcia-Ochoa & Gomez (2009) was used to determine the oxygen uptake rate (OUR) and  $OTR/K_{La}$ .

##### 2.6.1. Oxygen uptake rate

Five steps were followed to determine OUR (Garcia-Ochoa & Gomez 2009):

- i. Step one – the airflow into the aeration unit was turned off for 10 min, which was enough to prevent microorganisms from being starved of oxygen.
- ii. Step two – the decrease in DO concentration was monitored during the non-aeration period using a DO meter and probe.
- iii. Step three – the decrease in DO was plotted against time using Microsoft Excel.
- iv. Step four – a linear regression line was used to determine the rate of change in DO concentration with time. The rate of change in DO concentration was regarded as the OUR.
- v. Step five – Equation (2) defines the rate of change in DO concentration with time.

$$\frac{dC}{dt} = -q_{O_2}C_X \quad (2)$$

##### 2.6.2. Oxygen transfer rate/volumetric mass transfer coefficient

Seven steps were followed to determine  $OTR/K_{La}$  (Garcia-Ochoa & Gomez 2009).

- i. Step one – turn on the air supply in the aeration unit.
- ii. Step two – record the DO concentration at different time intervals.
- iii. Step three – measure the average DO concentration saturation in the biological aeration unit.
- iv. Step four – determine the natural logarithm of the difference between DO concentration at different time intervals and average DO concentration obtained at infinite time using Equation (3).

$$\ln(C^* - C) \quad (3)$$

v. Step five – determine the difference between time intervals using Equation (4).

$$(t_2 - t_1) \tag{4}$$

vi. Step six – produce a graph plot of Equations (3) and (4).

vii. Step seven – produce a linear regression line. The slope of the linear regression line is equal to the  $OTR/K_L a$ .

**2.6.3. Aeration efficiency**

Three steps were followed to determine AE (Garcia-Ochoa & Gomez 2009).

- i. Step one – determine  $OTR/K_L a$  in the aeration unit.  $OTR/K_L a$  will be determined as described in section 2.6.2.
- ii. Step two – determine the power used during the aeration process. Power input was determined as described in Table 1, using the digital wattmeter.
- iii. Step three – determine the AE. AE was determined by the quotient of  $OTR/K_L a$  and power input as described in Equation (1).

**2.6.4. Application of artificial neural network**

A regression model was developed using multilayer perceptron (MLP) artificial neural network (ANN) algorithm on MATLAB programming software. Continuous data collected from laboratory experiments was used to develop the AE model. The MLP ANN architecture is shown in Figure 2.

The general form of the MLP ANN algorithm is shown in Equation (5). Where  $X$  is the  $j$ th nodal value for the previous layer.  $Y$  is the  $i$ th nodal value in the current layer.  $f$  is the activation function.  $W_{ij}$  is the weighting factor, and  $b$  is the bias

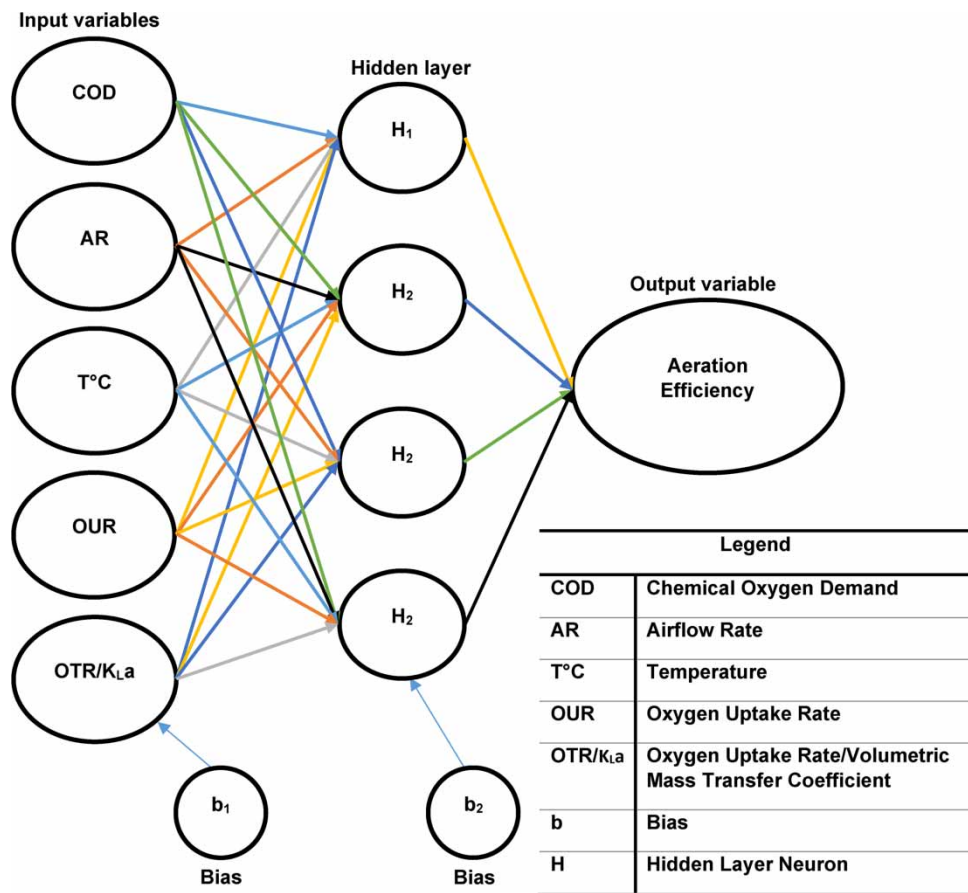


**Figure 2** | Aeration efficiency MLP ANN architecture.

of the  $i$ th node.

$$Y_i = f \left( \sum_{j=1}^N W_{ij} X_j + b_i \right) \quad (5)$$

Nine steps were followed to model AE using MLP ANN algorithm.

- The first step was to select input variables from the data collected during laboratory experiments.
- The second step was to split the data into 70% training, 15% validation, and 15% testing.
- The third step was to transform data into input variables using the normalization technique defined by Equation (6).

$$x(\text{scaled}) = \frac{x - \min_x}{\max_x - \min_x} \quad (6)$$

where  $x(\text{scaled})$  is the scaled sample data point,  $x$  is the sample data point,  $\min_x$  is the minimum value in the training dataset,  $\max_x$  is the maximum value on the training dataset.

- The fourth step was to select the MLP ANN architecture with one hidden layer and four neurons.
- The fifth step was to initialize the weights and bias between values of zero and one.
- The sixth step was to use the sigmoid activation function as a transfer function. The sigmoid function is defined by Equation (7) and Figure 3.

$$f = \frac{1}{1 + e^{-x}} \quad (7)$$

- The seventh step was to use the supervised gradient descent backpropagation learning algorithm to correct the weights and bias.
- The eighth step was to evaluate the performance of the AE model using MSE,  $R^2$ , and RMSE defined by Equations (8)–(10).

$$MSE = \sum_{i=1}^n \frac{(\hat{y}_i - y_i)^2}{N} \quad (8)$$

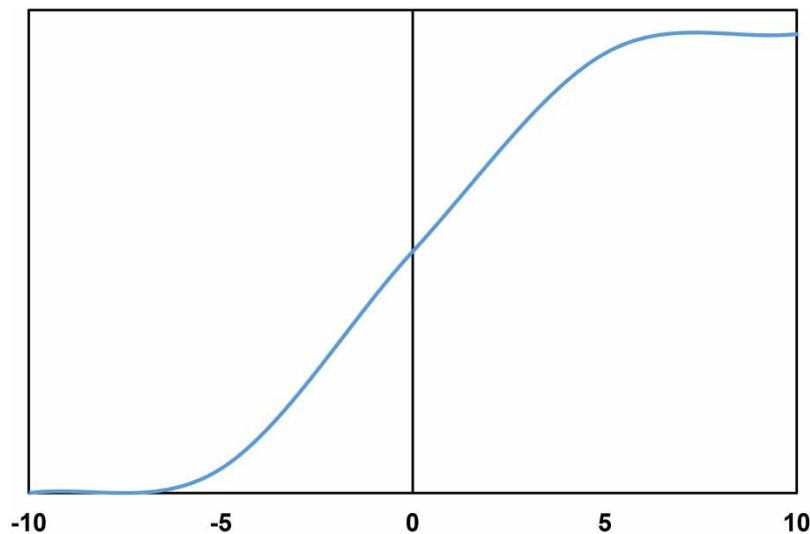


Figure 3 | Sigmoid Function.

$$R^2 = \frac{1}{m} \sum_{j=1}^m \left( 1 - \frac{SSE}{SST} \right) \quad (9)$$

$$RMSE = \sqrt{\frac{\sum_{i=1}^n (\hat{y}_i - y_i)^2}{N}} \quad (10)$$

where  $MSE$  is the mean squared error,  $\hat{y}_i$  is the predicted data,  $y_i$  is the observed data,  $N$  is the number of data points,  $R^2$  is the coefficient of determination,  $SSE$  is the sum of squared error, and  $SST$  is the total sum of squares.

- The ninth step was to perform sensitivity analysis on the AE model. A one factor at a time method was used. Each decision variable was individually adjusted by  $\pm 10\%$ ,  $\pm 20\%$ , and  $\pm 50\%$ , while keeping the others unchanged. In addition, decision variables were checked for their direct, inverse, major, or minor changes on AE.

### 3. RESULTS AND DISCUSSION

#### 3.1. Laboratory results

Table 2 presents Pearson correlation coefficient analysis results using a two tailed test at 95% significance while Figure 4(a)–(e) presents the relationship between AE and input parameters (COD, airflow rate, temperature, OUR, and OTR/ $K_La$ ). COD ( $-0.043^{**}$ ) produced a negative correlation relation to AE as shown in Table 2. This was because high concentrations of organic matter causes bubble coalescence in the biological treatment process. Bubble coalescence results in large bubbles that are faster, reducing contact time between air bubbles and wastewater. The less contact time between air bubbles and wastewater results in low AE, since the oxygen molecules carried by the air bubbles will not be able to penetrate wastewater thickness caused by high organic matter (Fan *et al.* 2014; Durán *et al.* 2016; Odize *et al.* 2017). Odize *et al.* (2017) reported that AE decreased by 0.47% with an increase in colloidal/particulate COD from 5 mg/L to 20 mg/L. Fan *et al.* (2014) reported a decrease of 1.744% in AE when the organic content increased from 2.840 g/L to 10.498 g/L in the biological activated sludge process. This can also be justified by the relationship between COD and OTR/ $K_La$  that produced a negative correlation of  $-0.579^{**}$ , which indicates that when COD increases, OTR/ $K_La$  decreases. The relationship between AE and COD shown in Figure 4(a) shows high AE at low COD concentration.

Airflow rate ( $-0.061^{**}$ ) produced a negative correlation relation to AE. At high airflow rates, air bubbles tend to move faster, resulting in a shorter retention time of air bubbles that contain oxygen in the biological treatment process. The shorter retention time means that less oxygen molecules will be absorbed in the wastewater, yet high power is being consumed, resulting in low AE (Ashley *et al.* 2008; Al Ba'ba'a *et al.* 2014; Collivignarelli *et al.* 2019). According to Ashley *et al.* (2008), an airflow rate of 10 L/min produced 270 kg O<sub>2</sub>/kWh AE, while an airflow rate of 40 L/min produced 180 kg O<sub>2</sub>/kWh AE. Similarly, Al Ba'ba'a *et al.* (2014) reported that an airflow rate of 14.4 L/min produced 64.05 kg O<sub>2</sub>/kWh AE while an airflow rate of 84 L/min produced 2.94 kg O<sub>2</sub>/kWh AE. Figure 4(b) shows a similar relationship between AE and airflow rate. This shows that high airflow rates are not beneficial in the biological treatment process. Temperature ( $0.575^{**}$ ) produced the highest

**Table 2** | Pearson correlation coefficient (2 tailed) between aeration efficiency and the parameters of interest

Correlation		Temperature	OUR	OTR/ $K_La$	COD	Airflow rate	AE
Temperature	Pearson Correlation	1					
OUR	Pearson Correlation	0.271**	1				
OTR/ $K_La$	Pearson Correlation	0.305**	0.747**	1			
COD	Pearson Correlation	0.123**	$-0.695^{**}$	$-0.579^{**}$	1		
Airflow rate	Pearson Correlation	0.000	0.097**	0.229**	0.008	1	
AE	Pearson Correlation	0.575**	0.206**	0.542**	$-0.043^{**}$	$-0.061^{**}$	1

\*\*Correlation is significant at the 0.01 level (2-tailed).

\*Correlation is significant at the 0.05 level (2-tailed).



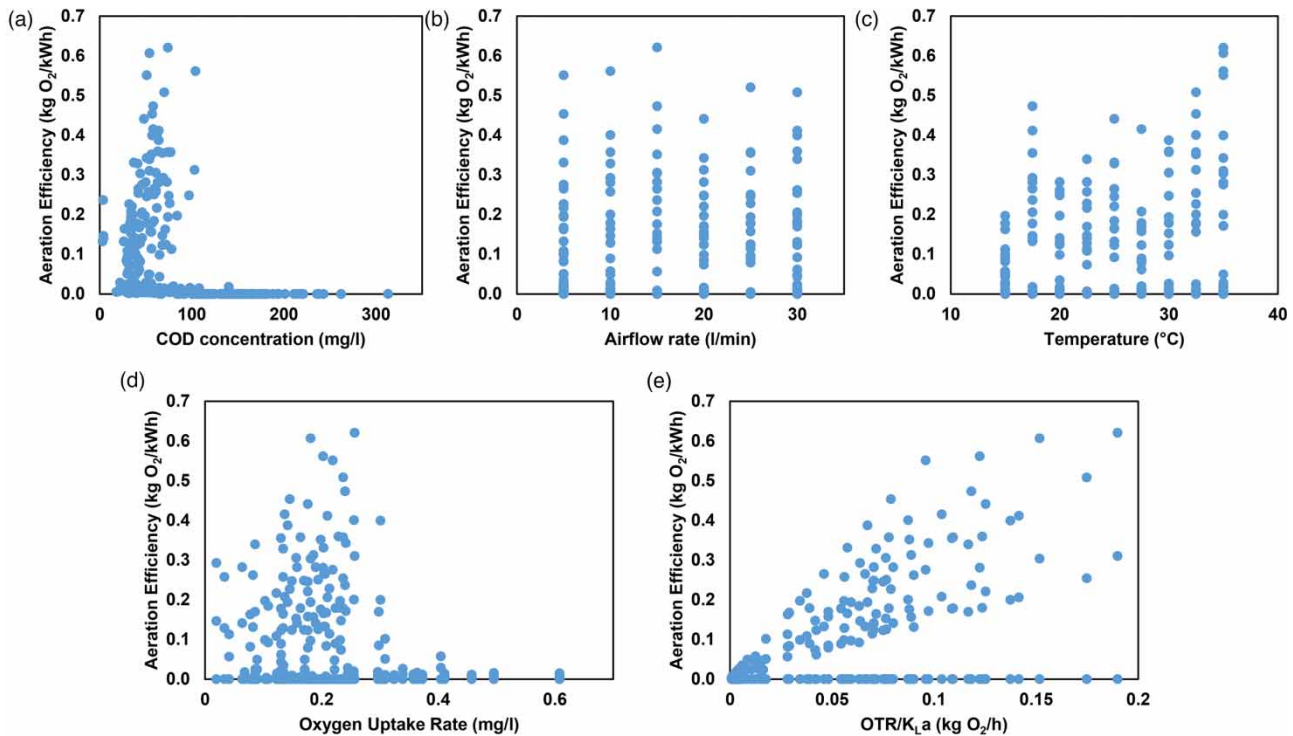


**Figure 4** | Relationship between aeration efficiency and COD (a), airflow rate (b), temperature (c), OUR (d), and OTR (e).

positive correlation relation to AE. This was because temperature controls the viscosity of wastewater, and at high temperatures the viscosity of wastewater is low, which increases the transfer of oxygen molecules in wastewater. When oxygen transfer is high in wastewater due to low viscosity, AE will increase because less power from air pumps/blowers is required to achieve high oxygen solubility (Therrien *et al.* 2019). This can also be justified by the relationship between temperature and OTR/K<sub>L</sub>a, which produced a positive correlation of 0.305\*\*. This relationship shows that when the viscosity of wastewater is low due to high temperatures, oxygen transfer increases due to a thin liquid film that allows for high oxygen transfer. Therrien *et al.* (2019) reported that a temperature of 10 °C produced 0.197 kg O<sub>2</sub>/kWh AE and a temperature of 30 °C produced 0.222 kg O<sub>2</sub>/kWh AE. This resulted in a 11.3% increase due to an increase in temperature of wastewater. The relationship between AE and temperature can be observed in Figure 4(c).

OUR (0.206\*\*) produced the third highest positive correlation relation to AE. In the biological treatment process, OTR/K<sub>L</sub>a is equal OUR when airflow rate is maintained at a constant because the rate of change in dissolved oxygen concentration remains the same. In addition, high OUR indicates high oxygen consumption by microorganisms, which suggests that oxygen was available in abundance due to high OTR/K<sub>L</sub>a, resulting in high AE. This can be justified by the relationship between OTR/K<sub>L</sub>a and OUR, which produced a positive correlation of 0.747\*\* in the biological treatment process. The graphical relationship between AE and OUR can be seen in Figure 4(d). OTR/K<sub>L</sub>a (0.542\*\*) produced the second highest positive correlation relation to AE. When OTR/K<sub>L</sub>a increases in the biological treatment process, it indicates that more mass of oxygen is being transferred into the wastewater using less power consumption, hence AE increases. In addition, OTR/K<sub>L</sub>a is directly proportional to AE as defined by Equation (1), hence they produce a positive relationship. The relationship between AE and OTR/K<sub>L</sub>a can be observed in Figure 4(e).

### 3.2. Modelling performance results

MLP ANN algorithm was successful in modelling AE in the biological treatment process. Figure 5 shows the 226 observed AE data that were used as input data during the training phase and the predicted AE data from the MLP ANN AE model during the training phase. The predicted data were close to the observed data, therefore MLP ANN algorithm was able to

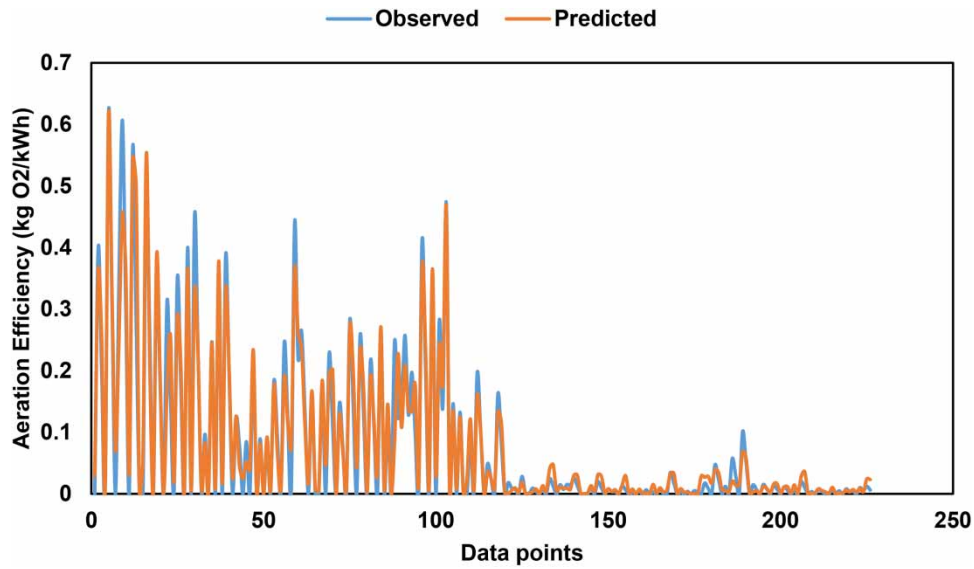


**Figure 5** | Observed vs predicted values during the training phase.

predict the AE data during the training phase. Overall performance of the model was acceptable since it was able to predict the maximum, middle, and minimum data points accurately.

Figures 6 and 7 show 49 observed data that were determined during the experiments and the predicted data from the MLP ANN algorithm during the validation and testing phase of the AE model, respectively. During the validation phase, the model predicted the minimum, middle, and maximum data accurately similar to the training phase. This means that the model generalised the data accurately as shown in Figure 6. Similarly, the model was able to predict the observed data during the testing phase. This means that the model was able to capture the observed data accurately as shown in Figure 7.

The prediction accuracy of the MLP ANN AE model was evaluated using  $R^2$ , RMSE, and MSE shown in Table 3. The optimum MSE of 0.00075 was determined during the validation phase of the AE model. The highest MSE of 0.0025 was determined during the testing phase of the model. Although the testing phase produced the lowest performance, the model performance was still acceptable. This means that the distance between the data points and the regression line are close to each other. The difference between the highest and lowest MSE was 70%, which was a significant difference. The relationship between MSE and number of iterations is shown in Figure 8. Similar results were obtained by the following scholars (Kundu *et al.* 2013; Tumer & Edebalı 2015; MG *et al.* 2018; Bekkari & Zeddouri 2019; Saleh & Kayı 2021). Saleh &

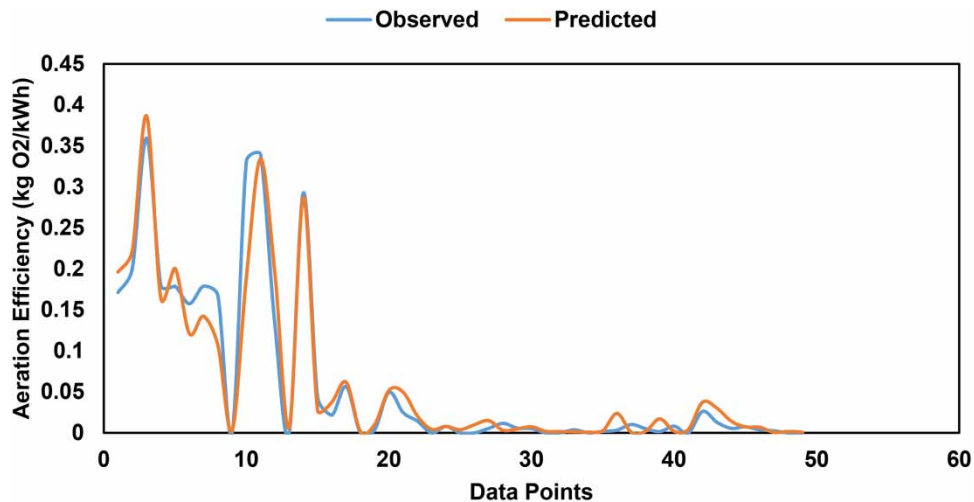


**Figure 6** | Observed vs predicted values during the validation phase.

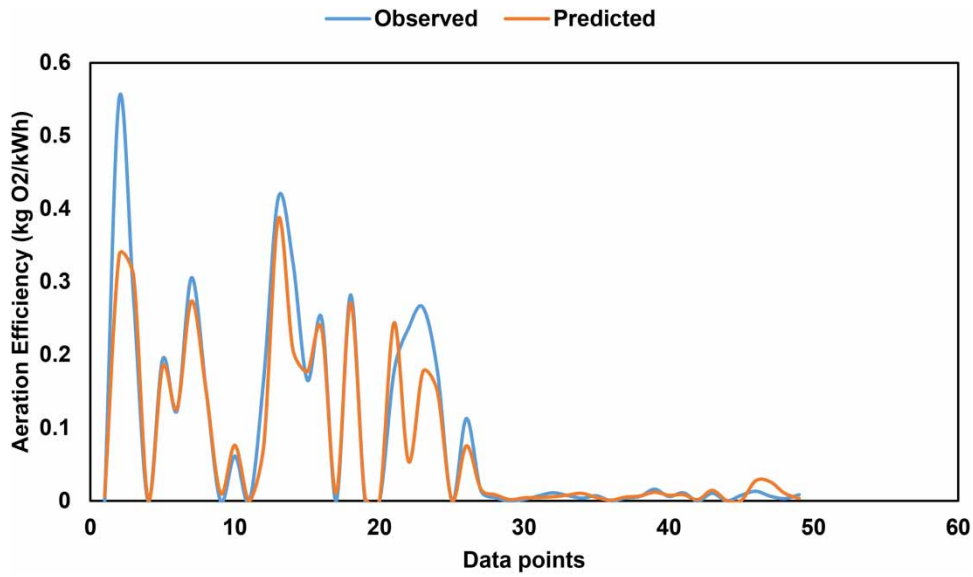


Figure 7 | Observed vs predicted values during the testing phase.

Table 3 | MLP ANN energy consumption model performance

	Training	Validation	Testing
R <sup>2</sup>	0.963	0.963	0.939
MSE	0.0012	0.00075	0.0025
RMSE	0.0353	0.0274	0.05

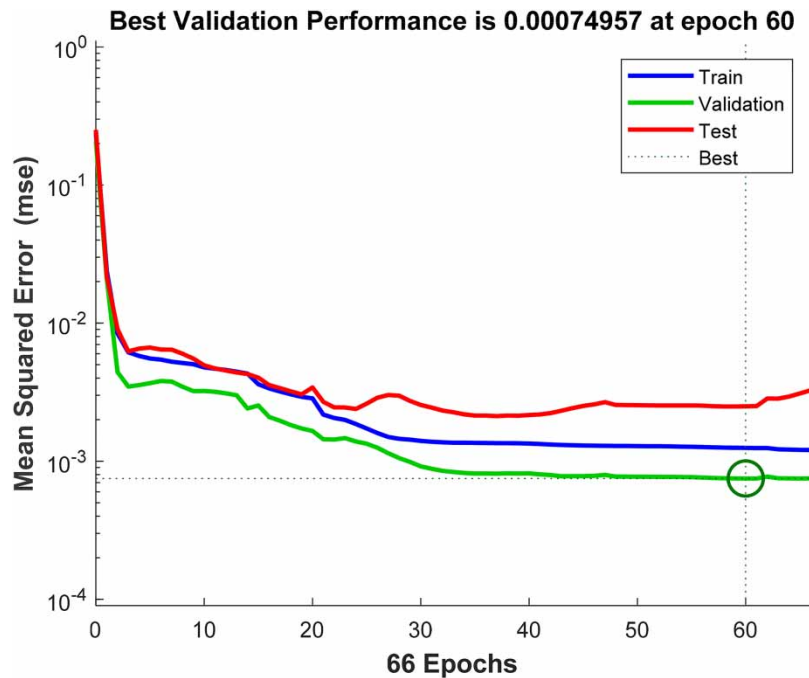


Figure 8 | Mean squared error performance at each iteration.

Kayi (2021) applied ANN algorithm to model the prediction of COD and the model produced MSE of 0.000441. MG *et al.* (2018) applied ANN algorithm in modelling WWTP performance and the model produced MSE value of 0.311. Similarly, Kundu *et al.* (2013) applied ANN algorithm to model the biological removal of organic carbon and nitrogen in wastewater and the model produced MSE of 2.81. Bekkari & Zeddouri (2019) applied ANN algorithm to predict effluent COD in wastewater and the model produced MSE of 0.056. Tumer & Edebali (2015) applied ANN algorithm to model the biological treatment process and the model produced MSE of 0.0041.

The blue, green, and red lines in Figure 8 indicate training, validation, and testing phases, respectively. The best line in Figure 8 indicates the lowest MSE and number of iterations during the validation phase of the model. Because the MSE was closer to zero during training, validation, and testing phases, it shows that the difference between the predicted and observed data was small. The results obtained in this study showed that MLP ANN algorithm captured the AE data accurately in the biological treatment process.

The RMSE during training, validation, and testing phase results were 0.0353, 0.0274, and 0.05, respectively, as shown in Table 3. The optimum RMSE was determined during the validation phase, which justifies the optimum MSE obtained during the validation phase. The difference between the highest and lowest RMSE was 29.4%, which was a significant difference. Overall, MLP ANN AE model performed well in all learning phases. Results obtained in this study were superior compared with the results obtained by other scholars (Hamada *et al.* 2018; Newhart *et al.* 2020; Aalami *et al.* 2021). Newhart *et al.* (2020) applied ANN algorithm to model acid disinfection performance in a WWTP and the model produced RMSE of 6.95. Similarly, Aalami *et al.* (2021) applied ANN algorithm to model the performance of a WWTP and the model produced RMSE of 3.93. Hamada *et al.* (2018) applied ANN algorithm to model the performance of a WWTP and the model produced RMSE of 29.69.

$R^2$  also showed good performance during training, validation, and testing phases. The training phase of the model produced  $R^2$  value of 0.962 as shown in Figure 9(a). This means that 96.2% of the data points fit the model accurately. Outliers are visible in Figure 9(a), which means that some of the data points did not fit the model accurately during the training phase. Validation phase produced  $R^2$  value of 0.923 as shown in Figure 9(b). This means that 92.3% of the data points fit the model accurately. Similar to the training phase, outliers were visible which means that some of the data points did not fit the model accurately. Testing phase produced  $R^2$  value of 0.939 as shown in Figure 9(c). This was a slight drop from the validation  $R^2$ . Overall, the AE model performance was acceptable.

Similar results were obtained by the following scholars (Kundu *et al.* 2013; Tumer & Edebali 2015; Hamada *et al.* 2018; Bekkari & Zeddouri 2019; Ofman & Struk-Sokolowska 2019; Oulebsir *et al.* 2020; Alsulaili & Refaie 2021). Alsulaili & Refaie (2021) applied ANN algorithm to model five day biological oxygen demand in wastewater treatment and the model produced  $R^2$  value of 0.754. Bekkari & Zeddouri (2019) applied ANN algorithm to predict effluent COD in wastewater and the model produced  $R^2$  of 88%. Ofman & Struk-Sokolowska (2019) applied ANN algorithm in modelling nitrogen forms in wastewater and the model produced  $R^2$  of 0.99. Oulebsir *et al.* (2020) modelled the activated sludge energy consumption.  $R^2$  values obtained were 94.41% and 82.42% during training and testing phases. Similarly, Tumer & Edebali (2015)

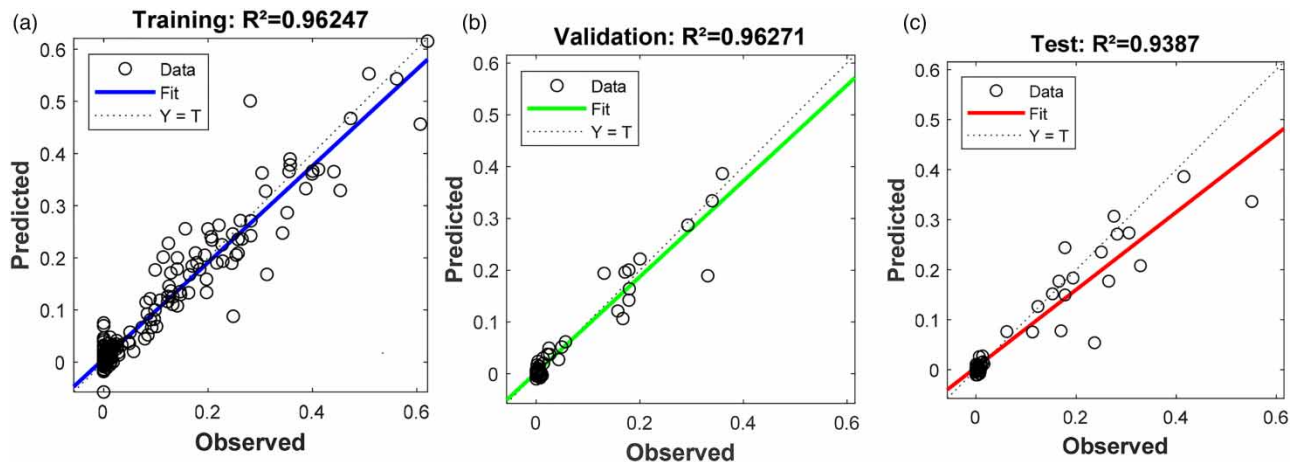


Figure 9 |  $R^2$  during training phase (a), validation phase (b), and testing phase (c).

applied ANN algorithm to model the biological treatment process and the model produced  $R^2$  of 96%. Kundu *et al.* (2013) applied ANN algorithm to model the biological removal of organic carbon and nitrogen in wastewater and the model produced  $R^2$  value of 96%. Hamada *et al.* (2018) applied ANN algorithm to model the performance of a WWTP and the model produced  $R^2$  of 78%.

### 3.3. Sensitivity analysis

Figure 10 presents the results of the AE model sensitivity analysis. The biggest driver of AE was temperature (34.6%). This was expected since temperature controls the viscosity of wastewater. COD (21%) was the second highest contributor to AE. This

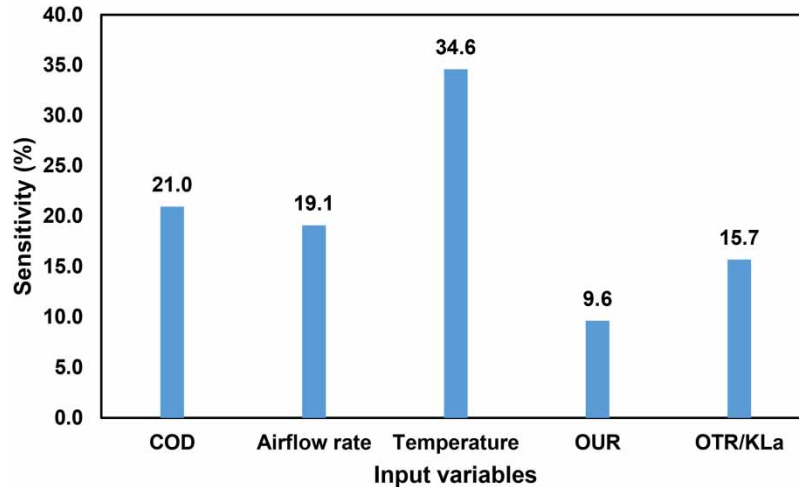


Figure 10 | Aeration efficiency model sensitivity analysis.

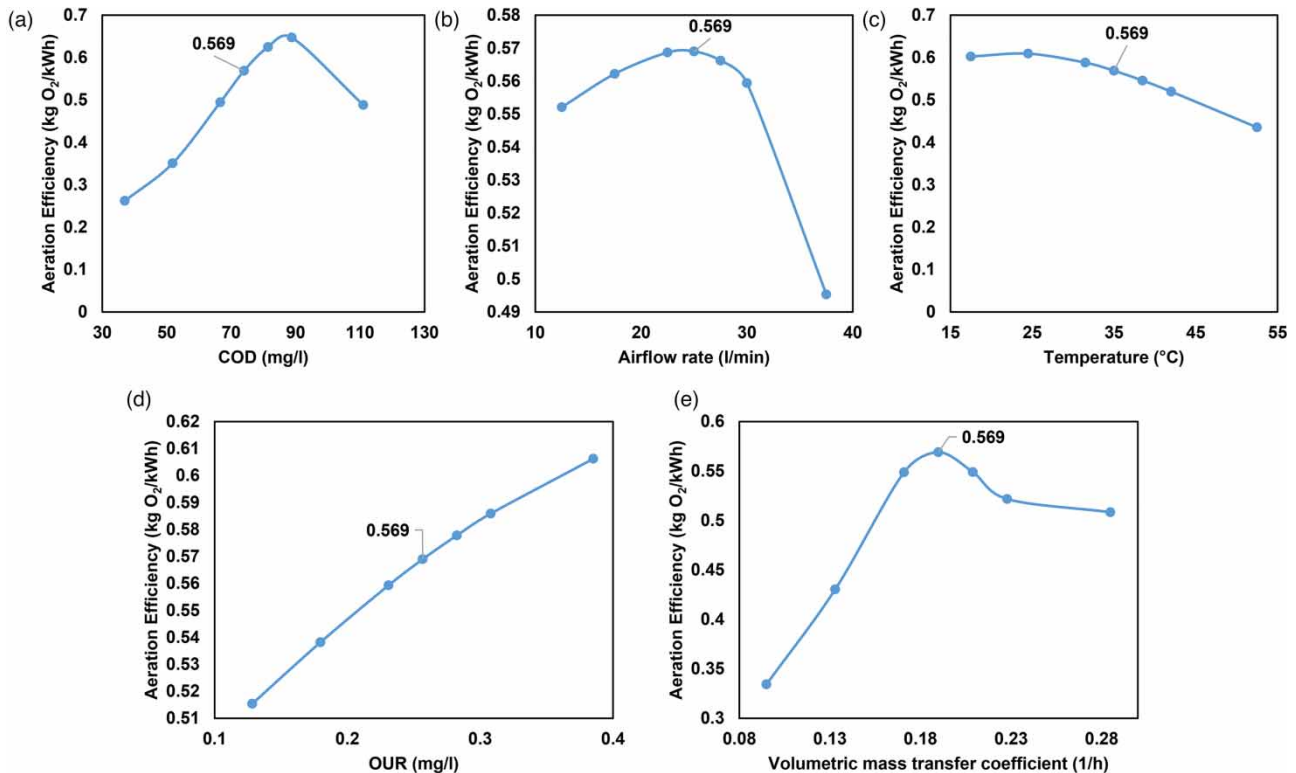


Figure 11 | Effect of COD (a), airflow rate (b), temperature (c), OUR (d), and OTR (e) on aeration efficiency.

was due to the fact that organic content creates impurities in wastewater, which will create a resistance of oxygen molecules to dissolve in the wastewater. Airflow rate (19.1%) and OTR/ $K_La$  (15.7%) contributed almost equally towards AE in the biological treatment process. The least contributor to AE model was OUR (9.6%). This implies that OUR can be eliminated as an input to predict AE. Temperature, COD, airflow rate, and OTR/ $K_La$  are more suitable as input variables in the AE model.

The relationships between each MLP ANN AE output results and input variables are presented in Figure 11. The input variables were controlled at 74 mg/L, 25 L/min, 35 °C, 0.2567 mg/L, and 0.1899/h for COD, airflow rate, temperature, OUR, and OTR/ $K_La$ , respectively. The control parameters produced an AE of 0.569 kg O<sub>2</sub>/kWh. The relationship between AE and COD concentration showed an increase of up to 88.8 mg/L, beyond that the AE decreased. This was because high COD concentrations decrease the ability of oxygen molecules to dissolve in the wastewater due to high impurities, resulting in low AE. Similarly, high airflow rates beyond 25 L/min affected AE, because high airflow rate consumes high power yet producing a moderate to high OTR/ $K_La$ , resulting in low AE in the biological treatment process. This shows that high airflow rates are not beneficial to improve AE. At high temperatures (30 °C and above) AE decreased. This suggests that the optimum operating temperature that allows for high AE was 30 °C. AE increased with an increase in OUR. This indicates that when OUR increases due to an increase in microorganisms, AE increases in the biological treatment process. AE increased with an increase in OTR/ $K_La$  up to 0.1899/h. Beyond OTR/ $K_La$  of 1,899/h, AE decreased.

#### 4. CONCLUSION

The aim of the study was to develop an AE model that can be used to monitor the performance of the biological treatment process. The following data collected from the laboratory was used: COD, temperature, airflow rate, OUR, and OTR/ $K_La$ . Low concentration of COD showed high AE. High AE was measured at low airflow rate of 15 L/min. High temperatures (35 °C) produced the highest AE of 0.621 kg O<sub>2</sub>/kWh. The highest AE (0.621 kg O<sub>2</sub>/kWh) was measured at moderate OUR of 0.2567 mg/l. AE increased with an increase in OTR/ $K_La$  in the biological treatment process. MLP ANN algorithm was used to model the AE data. MLP ANN algorithm was successful in modelling the AE data. R<sup>2</sup> values were 0.963, 0.963, and 0.939 for training, validation, and testing phases respectively. MSE values were 0.0012, 0.00075, and 0.0025 for the training, validation, and testing phases, respectively. RMSE values were 0.0353, 0.0274, and 0.05 for the training, validation, and testing phases, respectively. Sensitivity analysis showed that temperature (34.6%) and COD (21%) were the biggest drivers of AE in the biological treatment process. The AE model can be utilized by plant managers/operators to improve AE which ultimately improves energy consumption in the biological treatment process.

#### DATA AVAILABILITY STATEMENT

All relevant data are included in the paper or its Supplementary Information.

#### CONFLICT OF INTEREST

The authors declare there is no conflict.

#### REFERENCES

- Aalami, M. T., Hejabi, N., Nourani, V. & Saghebani, S. 2021 Investigation of artificial intelligence approaches capability in predicting the wastewater treatment plant performance (Case study: Tabriz wastewater treatment plant). *Amirkabir Journal of Civil Engineering* **53** (3), 15–15. doi:10.22060/CEEJ.2019.16757.6334.
- Al Ba'ba'a, H. B. & Amano, R. S. 2017 A study of optimum aeration efficiency of a lab-scale air-diffused system. *Water and Environment Journal* **31** (3), 432–439. <https://doi.org/10.1111/wej.12261>.
- Al Ba'ba'a, H. B., Prada, M. A., Olson, C. D., Alkhalidi, A. A., Amano, R. S. & Li, J. 2014 An experimental study of reducing back pressure of fine air diffuser used in wastewater plants. In: *ASME 2014 4th Joint US-European Fluids Engineering Division Summer Meeting Collocated with the ASME 2014 12th International Conference on Nanochannels, Microchannels, and Minichannels*. American Society of Mechanical Engineers, pp. V01CT16A006–V01CT16A006. <https://doi.org/10.1115/FEDSM2014-21203>.
- Alsulaili, A. & Refaie, A. 2021 Artificial neural network modeling approach for the prediction of five-day biological oxygen demand and wastewater treatment plant performance. *Water Supply* **21** (5), 1861–1877. <https://doi.org/10.2166/ws.2020.199>.
- American Public Health Association (APHA), American Water Works Association, Water Environment Federation 2012 *Standard Methods for the Examination of Water and Waste Water*, 22nd edn. American Public Health Association, Washington, DC, USA.
- Ashley, K. I., Mavinic, D. S. & Hall, K. J. 2008 Effect of orifice diameter, depth of air injection, and air flow rate on oxygen transfer in a pilot-scale, full lift, hypolimnetic aerator. *Canadian Journal of Civil Engineering* **36** (1), 137–147. <https://doi.org/10.1139/S08-047>.

- Baylar, A. & Bagatur, T. 2000 Aeration performance of weirs. *Water SA* **26** (4), 521–526. Available from: [https://hdl.handle.net/10520/AJA03784738\\_1609](https://hdl.handle.net/10520/AJA03784738_1609).
- Bekkari, N. & Zeddouri, A. 2019 Using artificial neural network for predicting and controlling the effluent chemical oxygen demand in wastewater treatment plant. *Management of Environmental Quality: An International Journal*. <https://doi.org/10.1108/MEQ-04-2018-0084>.
- Chalasan, G. & Sun, W. 2007 *Measurement of Temperature Effects on Oxygen Uptake Rate in Activated Sludge Treatment*. Report, Michigan State University College of Engineering, East Lansing, MI, USA, pp. 1–28. Available from: <http://citeseerx.ist.psu.edu/viewdoc/download?doi=10.1.1.529.6379&rep=rep1&type=pdf>.
- Christoforidou, P., Bariamis, G., Iosifidou, M., Nikolaidou, E. & Samaras, P. 2020 Energy benchmarking and optimization of wastewater treatment plants in Greece. In *Environmental Sciences Proceedings*. (Vol. 2, No. 1). Multidisciplinary Digital Publishing Institute, p. 36. <https://doi.org/10.3390/envirosci2020002036>.
- Collivignarelli, M. C., Abbà, A. & Bertanza, G. 2019 Oxygen transfer improvement in MBBR process. *Environmental Science and Pollution Research*, 1–11. <https://doi.org/10.1007/s11356-019-04535-1>.
- Du, Y., Chen, F., Zhou, L., Qiu, T. & Sun, J. 2020 Effects of different layouts of fine-pore aeration tubes on sewage collection and aeration in rectangular water tanks. *Aquacultural Engineering* **89**, 102060. <https://doi.org/10.1016/j.aquaeng.2020.102060>.
- Durán, C., Fayolle, Y., Pechaud, Y., Cockx, A. & Gillot, S. 2016 Impact of suspended solids on the activated sludge non-newtonian behaviour and on oxygen transfer in a bubble column. *Chemical Engineering Science* **141**, 154–165. <https://doi.org/10.1016/j.ces.2015.10.016>.
- Fan, H., Qi, L., Liu, G. H., Zhang, Y., Chen, X. & Wang, H. 2014 Promotion and inhibition of oxygen transfer under fine bubble aeration by activated sludge. *Water and Environment Journal* **28** (3), 434–441. <https://doi.org/10.1111/wej.12061>.
- García-Ochoa, F. & Gomez, E. 2009 Bioreactor scale-up and oxygen transfer rate in microbial processes: an overview. *Biotechnology Advances* **27** (2), 153–176. <https://doi.org/10.1016/j.biotechadv.2008.10.006>.
- Golzar, F., Nilsson, D. & Martin, V. 2020 Forecasting wastewater temperature based on artificial neural network (ANN) technique and monte carlo sensitivity analysis. *Sustainability* **12** (16), 6386. <https://doi.org/10.3390/su12166386>.
- Hamada, M., Adel Zaqoot, H. & Abu Jreiban, A. 2018 Application of artificial neural networks for the prediction of Gaza wastewater treatment plant performance-Gaza strip. *Journal of Applied Research in Water and Wastewater* **5** (1), 399–406. <https://doi.org/10.22126/arww.2018.874>.
- Kan, S. E., Fahmi, M. R., Shum, K. J., Ibrahim, A. H., Abidin, C. Z. A. & Kusuma, B. S. 2020 Improvement of oxygen transfer efficiency in the activated sludge process. In *IOP Conference Series: Earth and Environmental Science*. (Vol. 476, No. 1). IOP Publishing, Bristol, UK, p. 012098. Available from: <https://iopscience.iop.org/article/10.1088/1755-1315/476/1/012098/meta>.
- Kanaujia, D. K., Paul, T., Sinharoy, A. & Pakshirajan, K. 2019 Biological treatment processes for the removal of organic micropollutants from wastewater: a review. *Current Pollution Reports* **5** (3), 112–128. <https://doi.org/10.1007/s40726-019-00110-x>.
- Krahe, M., Antranikian, G. & Märkl, H. 1996 Fermentation of extremophilic microorganisms. *FEMS Microbiology Reviews* **18** (2–3), 271–285. <https://doi.org/10.1111/j.1574-6976.1996.tb00243.x>.
- Kundu, P., Debsarkar, A. & Mukherjee, S. 2013 Artificial neural network modeling for biological removal of organic carbon and nitrogen from slaughterhouse wastewater in a sequencing batch reactor. *Advances in Artificial Neural Systems* **2013**. <http://dx.doi.org/10.1155/2013/268064>.
- Lewis, W. K. & Whitman, W. G. 1924 Principles of gas absorption. *Industrial & Engineering Chemistry* **16** (12), 1215–1220. Available from: [chrome-extension://efaindbmnnnibpcajpcglcfeindmkaj/https://pubs.acs.org/doi/pdf/10.1021/ie50180a002?casa\\_token=qdjFqX6BgX4AAAAA:ZzX9w0NfZ9O4glg7yf7qAGxSHLauxuy-j9Amiz21Ymfh\\_kZhdPuY01CUf7QJPGzPIMkCA6-WIbiSdmQLlg](chrome-extension://efaindbmnnnibpcajpcglcfeindmkaj/https://pubs.acs.org/doi/pdf/10.1021/ie50180a002?casa_token=qdjFqX6BgX4AAAAA:ZzX9w0NfZ9O4glg7yf7qAGxSHLauxuy-j9Amiz21Ymfh_kZhdPuY01CUf7QJPGzPIMkCA6-WIbiSdmQLlg).
- Limpaiboon, K. 2013 Influence of operating conditions and physical properties of liquid medium on volumetric oxygen transfer coefficient in a dual impeller bioreactor. *Walailak Journal of Science and Technology (WJST)* **10** (6), 625–634. Available from: <https://103.58.148.28/index.php/wjst/article/view/472>.
- MG, H. N., Manilal, A. M., Anand, P. G. & Soloman, P. A. 2018 Artificial Neural Network Based Control of Electrocoagulation based Automobile Wastewater Treatment Plant. In *2018 International Conference on Circuits and Systems in Digital Enterprise Technology (ICCSDET)*. IEEE, pp. 1–4. doi:10.1109/ICCSDET.2018.8821131.
- Newhart, K. B., Goldman-Torres, J. E., Freedman, D. E., Wisdom, K. B., Hering, A. S. & Cath, T. Y. 2020 Prediction of peracetic acid disinfection performance for secondary municipal wastewater treatment using artificial neural networks. *ACS ES&T Water* **1** (2), 328–338. <https://doi.org/10.1021/acsestwater.0c00095>.
- Odize, V. O., Novak, J., De Clippeleir, H., Al-Omari, A., Smeraldi, J. D., Murthy, S. & Rosso, D. 2017 Reverse flexing as a physical/mechanical treatment to mitigate fouling of fine bubble diffusers. *Water Science and Technology* **76** (7), 1595–1602. <https://doi.org/10.2166/wst.2017.171>.
- Ofman, P. & Struk-Sokolowska, J. 2019 Artificial neural network (ANN) approach to modelling of selected nitrogen forms removal from oily wastewater in anaerobic and aerobic gsb process phases. *Water* **11** (8), 1594. <https://doi.org/10.3390/w11081594>.
- Oulebsir, R., Lefkir, A., Safri, A. & Bermad, A. 2020 Optimization of the energy consumption in activated sludge process using deep learning selective modeling. *Biomass and Bioenergy* **132**, 105420. <https://doi.org/10.1016/j.biombioe.2019.105420>.

- Pappenreiter, M., Sissolak, B., Sommeregger, W. & Striedner, G. 2019 Oxygen uptake rate soft-sensing via dynamic kLa computation: cell volume and metabolic transition prediction in mammalian bioprocesses. *Frontiers in Bioengineering and Biotechnology* **7**, 195. <https://doi.org/10.3389/fbioe.2019.00195>.
- Pittoors, E., Guo, Y. & Van Hulle, S. W. 2014 Oxygen transfer model development based on activated sludge and clean water in diffused aerated cylindrical tanks. *Chemical Engineering Journal* **243**, 51–59. <https://doi.org/10.1016/j.cej.2013.12.069>.
- Ren, J., Cheng, W., Wan, T., Wang, M. & Jiao, M. 2018 Effect of aeration rates on hydraulic characteristics and pollutant removal in an up-flow biological aerated filter. *Environmental Science: Water Research & Technology* **4** (12), 2041–2050. doi:10.1039/C8EW00231B.
- Rosso, D. & Stenstrom, M. K. 2006 Economic implications of fine-pore diffuser aging. *Water Environment Research* **78** (8), 810–815. <https://doi.org/10.2175/106143006X101683>.
- Saleh, B. A. & Kayi, H. 2021 Prediction of chemical oxygen demand from the chemical composition of wastewater by artificial neural networks. In *Journal of Physics: Conference Series*, (Vol. 1818, No. 1). IOP Publishing, Bristol, UK, p. 012035. Available from: <https://iopscience.iop.org/article/10.1088/1742-6596/1818/1/012035/meta>.
- Shukla, B. K. & Goel, A. 2018 Study on oxygen transfer by solid jet aerator with multiple openings. *Engineering Science and Technology, An International Journal* **21** (2), 255–260. <https://doi.org/10.1016/j.jestch.2018.03.007>.
- Siatou, A., Manali, A. & Gikas, P. 2020 Energy consumption and internal distribution in activated sludge wastewater treatment plants of Greece. *Water* **12** (4), 1204. <https://doi.org/10.3390/w12041204>.
- Suresh, S., Srivastava, V. C. & Mishra, I. M. 2009 Techniques for oxygen transfer measurement in bioreactors: a review. *Journal of Chemical Technology & Biotechnology: International Research in Process, Environmental & Clean Technology* **84** (8), 1091–1103. <https://doi.org/10.1002/jctb.2154>.
- Tejaswini, E., Babu, G. U. B. & Rao, A. S. 2020 Effect of temperature on effluent quality in a biological wastewater treatment process. *Chemical Product and Process Modeling* **15** (1). <https://doi.org/10.1515/cppm-2019-0018>.
- Therrien, J. D., Vanrolleghem, P. A. & Dorea, C. C. 2019 Characterization of the performance of venturi-based aeration devices for use in wastewater treatment in low-resource settings. *Water SA* **45** (2), 251–258. Available from: <https://hdl.handle.net/10520/EJC-15975b7367>.
- Tumer, A. E. & Edeballi, S. 2015 An artificial neural network model for wastewater treatment plant of Konya. *International Journal of Intelligent Systems and Applications in Engineering* **3** (4), 131–135. <https://doi.org/10.18201/ijisae.65358>.
- Vogelaar, J. C. T., Klapwijk, A., Van Lier, J. B. & Rulkens, W. H. 2000 Temperature effects on the oxygen transfer rate between 20 and 55 C. *Water Research* **34** (3), 1037–1041. [https://doi.org/10.1016/S0043-1354\(99\)00217-1](https://doi.org/10.1016/S0043-1354(99)00217-1).
- Wang, H., Yang, Y., Keller, A. A., Li, X., Feng, S., Dong, Y. N. & Li, F. 2016 Comparative analysis of energy intensity and carbon emissions in wastewater treatment in USA, Germany, China and South Africa. *Applied Energy* **184**, 873–881. <https://doi.org/10.1016/j.apenergy.2016.07.061>.
- Warunyuwong, P. & Imai, T. 2020 Study of air–water interface generator as oxygen transfer enhancer in diffused aeration system. *Environmental Technology*, 1–7. <https://doi.org/10.1080/09593330.2020.1830182>.
- Yang, H. C. & Park, S. K. 2012 Oxygen transfer characteristics of an ejector aeration system. *International Journal of Fluid Machinery and Systems* **5** (1), 10–17. <https://doi.org/10.5293/IJFMS.2012.5.1.010>.
- Zhou, Y., Han, L. R., He, H. W., Sang, B., Yu, D. L., Feng, J. T. & Zhang, X. 2018 Effects of agitation, aeration and temperature on production of a novel glycoprotein GP-1 by *Streptomyces kanasensis* ZX01 and scale-up based on volumetric oxygen transfer coefficient. *Molecules* **23** (1), 125. <https://doi.org/10.3390/molecules23010125>.
- Żyłka, R., Karolinczak, B. & Dąbrowski, W. 2021 Structure and indicators of electric energy consumption in dairy wastewater treatment plant. *Science of the Total Environment* **782**, 146599. <https://doi.org/10.1016/j.scitotenv.2021.146599>.

First received 15 August 2022; accepted in revised form 21 November 2022. Available online 25 November 2022